Journal of Catalysis **209,** 126–134 (2002)
doi:10.1006/jcat.2002.3606

Oxidation of CO on a Pt/Al_2O_3 Catalyst: From the Surface Elementary Steps to Lighting-Off Tests

III. Experimental and Kinetic Model for Lights-Off Tests in Excess CO

Abdennour Bourane and Daniel Bianchi[1]

Laboratoire d'Application de la Chimie à l'Environnement (LACE), UMR 5634, Université Claude Bernard, Lyon-I, Bat. 303, 43 Bd du 11 Novembre 1918, 69622 Villeurbanne, France

Received November 21, 2001; revised March 14, 2002; accepted March 14, 2002

The adsorption of CO (1% CO/He mixture) at 300 K on a 2.9% Pt/Al_2O_3 catalyst leads to the detection of a strong IR band at 2075 cm^{-1} associated with weak and broad IR bands in the range 1900–1700 cm^{-1} ascribed to linear (denoted L) and multibound (bridged and threefold coordinated) CO species, respectively. In parts I and II of the present study it was shown that the L CO species is oxidized at $T < 350$ K according to the surface elementary step denoted S3, $L + O_{wads} \rightarrow CO_2$, where O_{wads} is a weakly adsorbed oxygen species formed without competition with the L CO species by the dissociative chemisorption of O_2. In the present study the coverage of the L CO species as well as the conversion of CO into CO_2 are determined during the increase in the reaction temperature T_r from 300 to 740 K (lighting-off tests) using several 1% CO/x% O_2/He mixtures, with $x \leq 0.5$. In an excess of CO ($x < 0.5$), it is shown that the experimental curves $\theta_L = f(T_r)$ can be fitted by a kinetic model by considering that θ_L is determined by the equilibrium between the rates of adsorption, oxidation, and desorption of the L CO species. The parameters used in the kinetic model are those previously determined by studying (a) the adsorption equilibrium of the L CO species in the temperature range 300–740 K and (b) its oxidation by O_2 at $T < 350$ K (in the absence of CO). The evolution of the experimental turnover frequency (TOF_{ex}) during the increase in T_r is determined and compared to the theoretical TOF_{th} for low CO conversions. It is shown that $TOF_{ex} = f(T_r)$ is in very good agreement with a Langmuir–Hinshelwood mechanism via step S3, with the kinetic parameters used to fit the curves $\theta_L = f(T_r)$.

1. INTRODUCTION

In parts I (1) and II (2) of the present study we determined the kinetic parameters of the oxidation of the linear CO species (denoted L) formed on a 2.9% Pt/Al_2O_3 catalyst during adsorption of CO. Using FTIR spectroscopy (1) it has been shown that at $T < 350$ K, the L CO species (characterized by an IR band at ≈2075 cm^{-1}) is oxidized into CO_2 according to the Langmuir–Hinshelwood surface elementary step (denoted S3): $L + O_{wads} \rightarrow CO_2$. The rate of the reaction is $v_3 = -d\theta_L/dt = k_3\theta_L\theta_{O_{wads}}$, where $k_3 = A_3 \exp(-E_3/RT)$ is the rate constant and θ_L and $\theta_{O_{wads}}$ are the coverage of the L and O_{wads} species, respectively. This expression of the rate of reaction assumes that there is a uniform distribution of the adsorbed CO species, as discussed in part II (2), in relationship to the mobility of the adsorbed species. The main conclusions of part I are (a) there is no competition between the L and O_{wads} species, which are adsorbed on different sites, and (b) O_{wads} is weakly adsorbed, with a heat of adsorption $E_{O_2} < \approx 30$ kJ/mol. This leads to a rate for step S3 given by $v_3 = k_3\theta_L(K_{O_2}P_{O_2})^{0.5}$, where K_{O_2} and P_{O_2} are the adsorption coefficient and the partial pressure of oxygen, respectively. It has been determined (1) that $A_3 \approx 10^{13}$ s^{-1} at $T < 350$ K, with E_3 in the range (65–80) ± 5 kJ/mol. In part II (2) experiments in the transient regime with a mass spectrometer as a detector confirmed the conclusions of (1) and in addition C and O mass balances proved the presence of O_{wads} species on the Pt surface. Moreover, it was also observed that a strongly adsorbed oxygen species (denoted O_{sads}) is formed for each L CO species removed by oxidation (2). This O_{sads} species may oxidize the L CO species according to a surface elementary step (denoted step S3a), $L + O_{sads} \rightarrow CO_2$, but with a lower rate than step S3.

In the present study θ_L as well as the turnover frequency (TOF_{ex}) are determined during lighting-off tests using 1% CO/x% O_2/He mixtures ($x \leq 0.5$, excess CO). The experimental curves $\theta_L = f(T_r)$ as well as $TOF_{ex} = f(T_r)$ for low CO conversion values are interpreted by considering that the L CO species is the adsorbed intermediate species of the CO/O_2 reaction. The elementary steps involved in this reaction are Model M1, as follows.

Step S1 (formation of the L CO species):

$$CO_{(gas)} \Leftrightarrow L$$

[1] To whom correspondence should be addressed. E-mail: daniel.bianchi@univ-lyon1.fr.

0021-9517/02 $35.00

Step S2 (dissociative chemisorption of oxygen):

$$O_{2(gas)} \Leftrightarrow 2O_{wads}$$

Step S3 (oxidation of the L CO species):

$$L + O_{wads} \rightarrow CO_{2(ads)}$$

Step S4 (desorption of CO_2):

$$CO_{2(ads)} \rightarrow CO_{2(gas)}$$

These elementary steps are those usually considered to interpret the CO/O_2 reaction (3, 4) even if (a) step S2 is not always considered at equilibrium (3) and (b) the nature of the adsorbed CO species is not specified. The main objective of the present study is to show that Model M1 allows us to interpret the evolution of θ_L as well as of the TOF during the increase in T_r (lighting-off tests) in excess CO.

There are numerous studies in the literature with similar objectives (3–8). However, usually the authors develop a rate expression for the CO_2 production from an assumed mechanism and by optimization they fit the experimental data with their theoretical expressions (5, 6). This leads to the simultaneous determination of several kinetic parameters (i.e., activation energies, heats of adsorption). Another method consists of introducing the values of the kinetic parameters determined on single crystals in the various kinetic equations (7, 8). We develop a different approach because the elementary steps of model M1 have been studied individually in separate experiments. For instance, step S1 has been characterized (9–11) by studying the evolution of θ_L during the CO adsorption on Pt/Al_2O_3 at several adsorption pressures, P_a, and temperatures, T_a. The curves $\theta_L = f(T_a)$ at constant P_a values lead to the heats of adsorption of the L species at several θ_L values (denoted E_{θ_L}). Moreover, it has been observed that the E_{θ_L} values are not significantly modified in the presence of coadsorbed species in particular with CO/O_2 (for CO/O_2 ratios >2) and CO/CO_2 gas mixtures (12). Step S4 is considered fast (3). Steps S3 and correlatively step S2 were studied in parts I (1) and II (2). This approach of the kinetic modeling presents two main interests: (a) it fixes several kinetic parameters for the comparison of the experimental data with the various theoretical curves, and (b) it leads to new insights into the mechanism of the oxidation of CO on supported Pt catalysts.

2. EXPERIMENTAL

The preparation and characterization of the 2.9% Pt/Al_2O_3 (in weight percent γ-Al_2O_3) catalyst have been described in previous studies (1, 2, 9–13). For the FTIR study, the catalyst was compressed to form a disk ($\Phi =$ 1.8 cm; weight, ≈40–90 mg) which was placed in the sample holder of a small-internal-volume stainless steel IR cell (transmission mode) described elsewhere (9). This IR cell enabled *in situ* treatments (293–900 K) of the solid, at atmospheric pressure, with a gas flow rate in the range of 150–2000 cm^3/min. The same disk of catalyst was used for several experiments, and before the CO adsorption or the CO/O_2 reaction, it was treated *in situ* (150 cm^3/min) at 713 K according to the following procedure: oxygen (30 min) → helium (30 min) → hydrogen (1 h) → helium (10 min) → helium (adsorption or reaction temperature). The Pt dispersion of a fresh catalyst progressively reduced according to the procedure described in (13) was 0.85. However, to stabilize the Pt dispersion at 0.6–0.5, the solid was heated in 1% CO/He from 300 to 713 K before the experiments with CO/O_2 mixtures (1, 2, 9–12).

The data during either adsorption of CO or a lighting-off test were obtained according to the following procedure: after the pretreatment of the stabilized solid, a 1% CO/x% O_2/He mixture (total pressure = 1 atm, $x \leq 0.5$, flow rate = 200 cm^3/min) was introduced into the IR cell at 300 K and T_r was slowly increased (≈5–10 K/min) up to 740 K while simultaneously the FTIR spectra of the adsorbed species were recorded periodically. Then the solid was cooled in the presence of the reactive mixture and the FTIR spectra were compared to those recorded at similar temperatures in the course of the heating stage. Other authors have performed similar experiments at lower temperatures on supported Pt catalysts, in particular Kaul and Wolf (14, 15), Anderson (16), Haaland and Williams (17), Barshad *et al.* (18), and Lindstrom and Tsotsis (19) (see also the part dedicated to the CO/O_2 reaction in the review of Schüth *et al.* (20) on the oscillation regimes). However, the authors focused mainly on experimental conditions in excess O_2, which led to surface processes different from that observed in excess CO. During lighting-off tests, the disappearance of CO and the appearance of CO_2 were determined by the analysis of the gas mixture at the outlet of the IR cell using a second FTIR spectrometer with an IR gas cell ($L = 20$ cm; volume, 200 cm^3).

In parallel to the FTIR study, lighting-off tests were performed in a quartz microreactor (powder of catalyst) using experimental conditions similar to the study of Cai *et al.* (21) (weight of catalyst, ≈200 mg; flow rate in the range 100–600 cm^3/min). The composition (in molar fraction) of the gas mixtures at the outlet of the reactor and the temperature of the catalyst (using a small K thermocouple inserted in the catalyst powder) was determined with a mass spectrometer according to a procedure previously described (2).

3. RESULTS AND DISCUSSION

3.1. Coverage and Heats of Adsorption of the L Species during CO Adsorption

The FTIR results observed in the absence of O_2 in the course of the increase in the adsorption temperature, T_a, as well as the procedure to determine the heats of adsorption

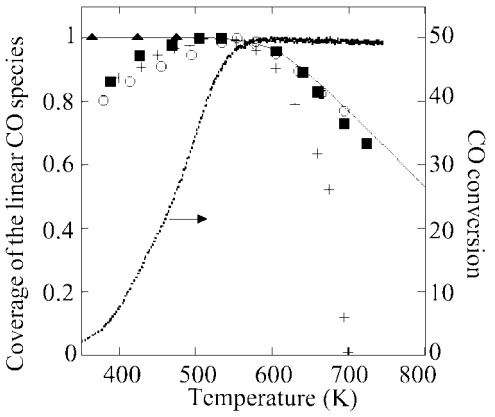

FIG. 1. Evolution of the coverage of the L CO species on Pt/Al_2O_3 with the temperature for various 1% CO/x% O_2/He mixtures: (circles, triangles) $x = 0$, heating and cooling stage, respectively; (solid line) theoretical coverage for $x = 0$; (■) $x = 0.125$; (+) $x = 0.5$; (dotted line) CO conversion with $x = 0.25$.

have been previously described in detail (9–11). However, we summarize below the main results to facilitate the comparison with the results observed in the presence of O_2. We have studied (9–11) the shift of the IR band of the L CO species and the evolution of its area, increasing T_a with 1% CO/He. The value of θ_L at T_a was obtained (9–11) using the ratio between the IR band area at T_a and the highest IR band area (at $T_a \approx 540$ K), as justified in (13). The circles in Fig. 1 show the evolution of θ_L with the increase in T_a. The increase in θ_L observed between 300 and 520 K has been attributed to the irreversible reconstruction of the Pt/CO system (9–11). For instance the triangles in Fig. 1 (curve obtained from cooling of the solid from 520 K) show that the coverage remains constant. The circles (Fig. 1) show that θ_L is constant between $T_a \approx 520$ and 600 K and finally decreases according to a straight line in a wide range of temperatures.

The curve $\theta = f(T_a)$ at the partial pressure $P_a = 10^3$ Pa has been used for the determination of the heats of adsorption of the L species using an adsorption model (9–11). This model assumes that (a) the L species is localized and (b) its heat of adsorption linearly decreases with increase in θ_L. Assumption (a) permits consideration of the fact that the adsorption coefficient is given by the statistical thermodynamics (22, 23),

$$K = \frac{h^3}{k \cdot (2 \cdot \pi \cdot m \cdot k)^{3/2}} \cdot \frac{1}{T_a^{5/2}} \cdot \exp\left(\frac{E_d - E_a}{R \cdot T_a}\right), \qquad [1]$$

where h is Planck's constant, k is Bolztmann's constant, m is the mass of the molecule (28×10^{-3} kg/6.02×10^{23}), E_d and E_a are the activation energies of desorption and adsorption, respectively, and $E_d - E_a$ is the heat of adsorption (denoted E). Assumption (b) leads to an expression of the coverage for an adsorbed species given by (9–11, and references therein)

$$\theta_L = \frac{RT_a}{\Delta E} \cdot \ln\left(\frac{1 + K_0 \cdot P_a}{1 + K_1 \cdot P_a}\right), \qquad [2]$$

where ΔE is the difference in the heats of adsorption at $\theta = 0$ (E_0) and $\theta = 1$ (E_1), K_0 and K_1 are the adsorption coefficients at $\theta_L = 0$ and $\theta_L = 1$, and P_a is the adsorption pressure. For the determination of E_1 and E_0 we only have to find the values to be used in [1] and [2] to obtain the best fit between experimental and theoretical coverage values. For instance, the solid line in Fig. 1 is obtained using $E_0 = 206$ kJ/mol and $E_1 = 115$ kJ/mol in expressions [1] and [2]. It shows the very good agreement between the theoretical coverage and the experimental data. The above heat of adsorption values are in agreement with certain literature data (10, 11) and with the isosteric heat of adsorption (10).

3.2. Coverage of the Linear CO Species and CO Conversion in the Presence of O_2 for CO/O_2 Ratios ≥2

Figure 2 shows the evolution of the IR band of the L species in the presence of 1% CO/0.125% O_2/He with the increase in T_r. The results are very similar to those observed with the 1% CO/He mixture (9–11). At low temperatures (Fig. 2a) the IR band is detected at the same position (2073 cm^{-1}) as that observed in the absence of O_2 associated with the detection of a shoulder at 2085 cm^{-1}, which is observed at higher temperatures with 1% CO/He (9–11). Note the presence of a very weak IR band at ≈2120 cm^{-1} due to the adsorption of CO on Pt^{2+} sites not observed in the absence of O_2 (9–11). For $T < 510$ K the intensity of the IR band increases (Figs. 2a–2c) with the increase in T_r while a shift is observed to lower wavenumbers (2063 cm^{-1} at $T = 503$ K). Between 510 and 570 K, the intensity of the

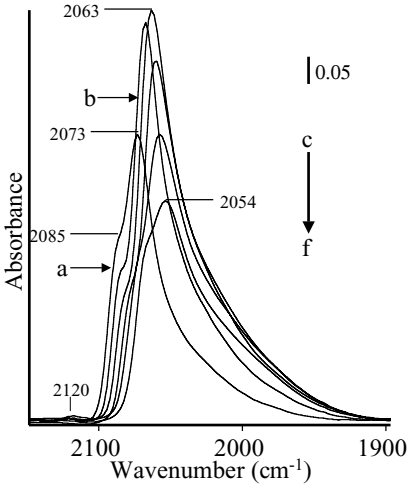

FIG. 2. FTIR spectra recorded at various temperatures in the course of a lighting-off test with the 1% CO/0.125% O_2/He mixture on Pt/Al_2O_3: (a–f) 351, 388, 503, 603, 663, and 723 K.

IR band remains constant and for higher temperatures a progressive decrease is observed associated with a shift to lower wavenumbers (2062, 2058, and 2054 cm^{-1} for 603, 663, and 723 K, respectively). Moreover, the analysis of the gas mixture at the outlet of the IR cell indicates that CO is oxidized into CO_2 during the increase in T_r. At the highest temperature ($T = 723$ K) and with a 200 cm^3/min flow rate the CO conversion (50%) corresponds to that expected for the total conversion of O_2 (Fig. 1, dotted line). It must be noted that at this temperature the support alone may also oxidize CO, as observed by other authors (21), but with a very low conversion (1.5% at 740 K with 1% CO/0.25% O_2/He). The θ_L value at the reaction temperature T_r with the 1% CO/0.125% O_2/He mixture (Fig. 1) is obtained using the ratio (IR band area at T_r)/(IR band area at 540 K). For $T_a < 510$ K, the increase in the curve $\theta_L = f(T_a)$ is probably due to the restructuring of the CO/Pt surface system, as observed with 1% CO/He. For $T > 570$ K, it can be observed that the curve of squares in Fig. 1 is only slightly lower than the curve of circles, which was obtained in the absence of oxygen. This leads to the conclusion that (a) the heat of adsorption of the linear CO species is not significantly modified by the presence of oxygen, as previously observed in (12), and (b) the CO/O_2 reaction does not strongly disturb the adsorption equilibrium for $T_r < 720$ K. We have performed similar experiments with 1% CO/0.25% O_2/He without observing significant differences in the FTIR spectra (Fig. 3) compared with 1% CO/0.125% O_2/He. The curve $\theta_L = f(T_r)$ with $P_{O_2} = 250$ Pa is only slightly lower than the curve of squares in Fig. 1 for $T_r > 630$ K (see Fig. 6). The decrease in T_r from 720 to 300 K in the presence of 1% CO/x% O_2/He mixtures ($x < 0.5$) leads to curves $\theta_L = f(T_r)$ (not shown), which overlap the curves obtained during the heating step (there are no hysteresis). The CO conversion

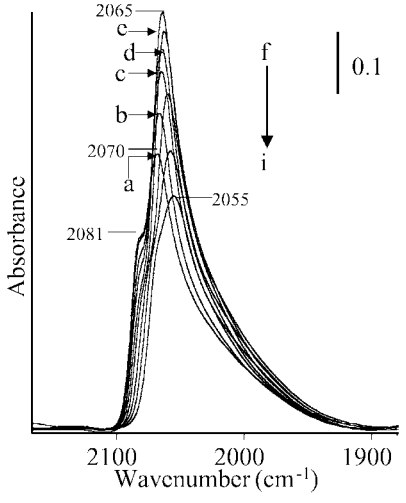

FIG. 3. FTIR spectra recorded at various temperatures in the course of a lighting-off test with the 1% CO/0.25% O_2/He mixture on Pt/Al_2O_3: (a–i) 345, 393, 448, 483, 543, 573, 633, 668, and 708 K.

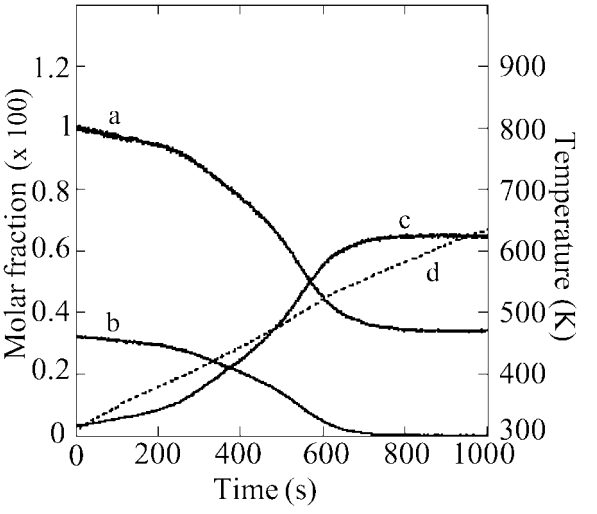

FIG. 4. Evolutions of the molar fractions and of T_r during a lighting-off test on Pt/Al_2O_3 with 1% CO/0.32% O_2/He: (a) CO; (b) O_2; (c) CO_2 (×100); (d) reaction temperature.

with the 1% CO/0.25% O_2/He mixture is reported as a dotted line in Fig. 1.

Figure 4 gives the evolution of the composition of the gas mixture at the outlet of the quartz microreactor and the temperature of the catalyst during a lighting-off test using a 1% CO/0.32% O_2/He mixture. It can be observed that the CO_2 production progressively increases with the increase in T_r in parallel to the decrease in CO and O_2. At high temperatures, the total amount of O_2 in the reactive mixture is consumed while the molar fractions of CO and CO_2 are those expected for the CO/O_2 reaction. Note that there is no major change in the increase in the temperature at high CO conversions due, for instance, to exothermic reactions: the temperature follows the programmed linear increase.

Figure 5 provides the FTIR spectra recorded during the increase in T_r with a 1% CO/0.5% O_2/He mixture. At 320 K the IR band is detected at 2073 cm^{-1} together with a shoulder at 2085 cm^{-1}. For $T_r < 560$ K (Figs. 5a–5c), there is strong similitude in the evolution of the FTIR spectra with that in Fig. 3. The main IR band shifts to lower wavenumbers (2073 and 2065 cm^{-1} at 326 and 538 K, respectively) while its intensity increases. The shoulder at 2085 cm^{-1} shifts to lower wavenumbers and is no longer detected at $T_r = 538$ K. For $T_r > 538$ K (Figs. 5d–5j) there is a clear difference in the results observed with lower P_{O_2} values: the IR band strongly decreases and disappears at 623 K associated with a shift to lower wavenumbers (2065, 2057, and 2054 cm^{-1} at 560, 585, and 603 K). Between 603 and 623 K the IR band is detected at the same position. It must be noted that the IR band strongly decreases in a short range of temperatures (585–623 K) but this decrease can be experimentally followed. The evolution of θ_L with T_r is shown in the curve of plus signs in Fig. 1. By comparison with the curve of circles it can be

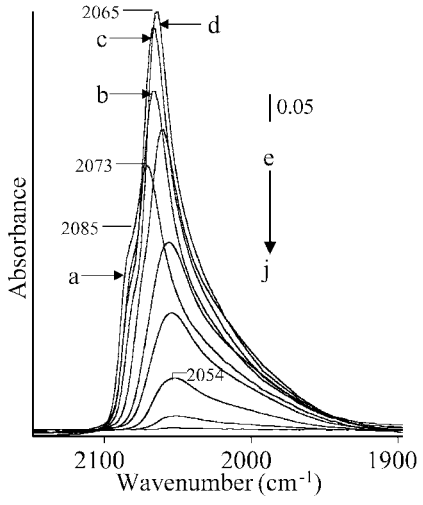

FIG. 5. FTIR spectra recorded at various temperatures in the course of a lighting-off test with the 1% CO/0.5% O_2/He mixture: (a–j) 326, 438, 470, 538, 585, 603, 608, 613, 618, and 623 K.

observed that the oxidation reaction strongly modifies the adsorption equilibrium with the 1% CO/0.5% O_2/He mixture. This is also observed for higher O_2 partial pressures. However, in that case, the coverage of the L CO species decreases from ≈1 to ≈0 in few degrees (<4 K), as observed by other authors (14, 17, 19).

3.3. Determination of the Theoretical Coverage of the L Species during a Lighting-Off Test

Model M1 of the Introduction is used to determine the theoretical coverage of the L species during the lighting-off tests. Following previous work on the heats of adsorption of the L species (10, 11), we consider that there is an equilibrium at each reaction temperature, T_r, between the rate of adsorption (denoted v_a) and the two rates of desorption (denoted v_d) and of oxidation (denoted v_o):

$$v_a - v_d - v_o = 0. \quad [3]$$

In parts I (1) and II (2), studying step S3 has shown that there is no competition between L and O_{wads} species, which are adsorbed on different sites. We have suggested that those sites are liberated by the desorption of the bridged CO species (1, 2), which has a low heat of adsorption (11). This leads to

$$k_a P_{CO}(1 - \theta_L) - k_d\theta_L - k_3\theta_{O_{wads}}\theta_L = 0, \quad [4]$$

where P_{CO} is the partial pressure of CO, k_a and k_d are the rate constants of adsorption and desorption, respectively, and θ_L and $\theta_{O_{wads}}$ are the coverages of the L and O_{wads} species, respectively. Expression [4] leads to

$$\theta_L = \frac{K_{CO} \cdot P_{CO}}{1 + K_{CO} \cdot P_{CO} + K_{ox} \cdot \theta_{O_{wads}}}, \quad [5]$$

where $K_{CO} = k_a/k_d$ is the adsorption coefficient for the L species given by expression [1] and K_{ox} is given by

$$K_{ox} = k_3/k_d, \quad [6]$$

which we define as an oxidation coefficient by analogy with the adsorption coefficient. The coverage $\theta_{O_{wads}}$ is given by Langmuir's model for dissociative chemisorption,

$$\theta_{O_{wads}} = \frac{\sqrt{K_{O_2} \cdot P_{O_2}}}{1 + \sqrt{K_{O_2} \cdot P_{O_2}}}, \quad [7]$$

where K_{O_2} is the adsorption coefficient of the O_{wads} species (given by [1] with $m = 32 \times 10^{-3}$ kg/6.02×10^{23}). In part I (1), we showed that the heat of adsorption of O_{wads} is $E_{O_2} \leq 30$ kJ/mol and that $(K_{O_2} \cdot P_{O_2})^{1/2} \ll 1$. Expression [7] gives $\theta_{O_{wads}} = (K_{O_2} \cdot P_{O_2})^{1/2}$, which is introduced in expression [5]. However, expression [5] derives from Langmuir's model for the CO adsorption, which is obtained by considering $\theta_{O_{wads}} = 0$ in [5] ($P_{O_2} = 0$). It has been previously shown (9–11) that this model does not represent the experimental data during the CO adsorption because the heat of adsorption linearly increases with the decrease in θ_L, as shown above by expression [2], which leads to the solid line in Fig. 1 with $E_0 = 206$ kJ/mol and $E_1 = 115$ kJ/mol. However, it is difficult to involve in a single step the mathematical treatments used to obtain expressions [2] and [5]. An alternative method must be used to involve simultaneously the linear increase in the heat of adsorption of the L species with the decrease in θ_L and the rate of oxidation of the L species. It has been previously shown on Pt- (10) and Pd- (24) supported catalysts that the heats of adsorption of CO at several coverages can be well estimated by considering Langmuir's model, with the adsorption coefficient given by expression [1], and by assuming that the heat of adsorption changes at each coverage. This approach has been suggested in early works (22, 23). For instance, curve a in Fig. 6 (same as solid line in Fig. 1) is obtained using expression [2]. Curve b in Fig. 6, which overlaps curve a, is obtained by considering in expression [5] that $\theta_{O_{wads}} = 0$ (adsorption experiment) and that the heat of adsorption of the L species linearly varies with θ_L from $E'_0 = 195$ kJ/mol to $E'_1 = 122$ kJ/mol. These values are in reasonable agreement with $E_0 = 206$ kJ/mol and $E_1 = 115$ kJ/mol, determined with expression [2] to obtain Fig. 6a. During a lighting-off test with CO/O_2 gas mixtures, θ_L is obtained from expression [5] by considering that the various kinetic parameters are those determined by studying each elementary step (1, 2, 9–11) as summarized below.

(a) The adsorption coefficient K_{CO} of the L species is given by expression [1], with the heat of adsorption of CO linearly varying from $E'_0 = 195$ kJ/mol at $\theta = 0$ to $E'_1 = 122$ kJ/mol at $\theta = 1$ (9–11, and present study).

(b) The rate constant of desorption of the L species is given by $k_d = (kT/h)\exp(-E_d/RT)$, with E_d varying with

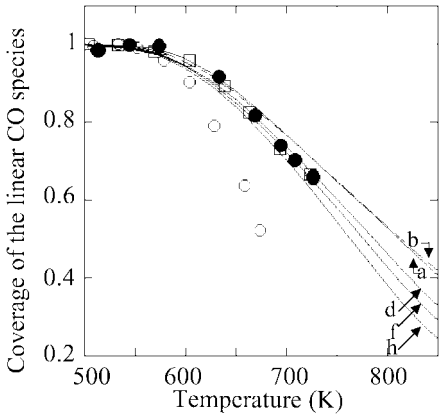

FIG. 6. Kinetic modeling of the coverage of the L species for CO/O_2 ratios ≥ 2: — (a), theoretical values using expression [2]; – – (b), theoretical coverage using Langmuir's equation; □ (c) and (solid line d) experimental data and theoretical coverages, respectively, for the 1%CO/0.125%O_2/He mixture; ● (e) and (solid line f) experimental data and theoretical coverages, respectively, for the 1%CO/0.25%O_2/He mixture; ○ (g) and (solid line h) experimental data and theoretical coverages respectively for the 1%CO/0.5%O_2/He mixture.

the coverage as the heat of adsorption (the CO adsorption is considered not activated).

(c) The adsorption coefficient K_{O_2} of the O_{wads} species is given by expression [1], with $E_{O_2} = 30$ kJ/mol (1).

(d) The oxidation coefficient K_{Ox} is given by expression [6], with $k_3 = (kT/h)\exp -(E_3/RT)$. The value of the activation energy E_3 is selected to obtain the best fitting between theoretical and experiment values by considering the range (65–80) $\pm$ 5 kJ/mol determined in (1). Note that the preexponential factor (s^{-1}) which was determined in (1) is in agreement with those used in several studies on kinetic modeling, e.g., 1×10^{13} (7), 1.2×10^{14} (25), 1×10^{12} (26), and 5.8×10^{13} (27), but significantly differs from other studies, e.g., 2×10^4 (28) and 2.7×10^6 (29).

(e) The partial pressure of CO is $P_{CO} = 1000$ Pa while that of O_2 is $P_{O_2} = 125$–500 Pa.

These various kinetic parameters are introduced in expression [5] and a numerical method determines the values of θ_L at each temperature T_r.

3.4. Comparison between Experimental and Theoretical Coverage of the L CO Species during a Lighting-Off Test for CO/O_2 Ratios $\geq$2

Curve d in Fig. 6 is obtained considering $P_{O_2} = 125$ Pa in expression [5] with $E_3 = 85$ kJ/mol. A good agreement can be observed between the theoretical curve (Fig. 6d) and the experimental data (Fig. 6c). E_3 values in the range 85 $\pm$ 2 kJ/mol give curves also in reasonable agreement with the experimental data. For $T > 600$ K, curve d shows that θ_L during the lighting-off test only slightly differs from the adsorption experiment (Fig. 6b). Curve f is obtained with the same kinetic parameters by considering $P_{O_2} = 250$ Pa and a good agreement with the experimental data (curve e) is also observed. For CO/O_2 ratios >2 it must be concluded that Model M1 and the kinetic parameters determined by individually studying each elementary step give a good representation of the evolution of θ_L during lighting-off tests. It is important to note that the decrease in θ_L for 550 K < T_r < 750 K is mainly due to the adsorption equilibrium (heat of adsorption) and not to step S3. Roughly during the CO/O_2 reaction in excess CO the coverage of the L CO species is determined by the adsorption equilibrium. Moreover, the good agreement between kinetic model and experimental data even when θ_L decreases due to the adsorption equilibrium clearly indicates that (a) this process does not significantly increase the amount of O_{wads} species on the surface, and (b) the kinetic model without competition between L and O_{wads} is still valid. This means that the coverage of the sites adsorbing the L species can decrease (in the range 1–0.6) without any significant effect on the rate of oxidation while it has been shown (2) that a strongly adsorbed oxygen species, O_{sads}, is formed for each L CO species removed from the surface. However, it has been shown that the O_{sads} species reacts with the L CO species according to surface elementary step S3a but with a rate significantly lower than step S3 (2). This explains that step S3a has no impact on the coverage of the L CO species during the CO/O_2 reaction. Curve h in Fig. 6 is obtained, similarly to curves d and f, by considering $P_{O_2} = 500$ Pa. Now, it can be observed that the theoretical curve h significantly differs from the experimental curve g. One of the possible explanations is that there is a mass transfer limitation. However, curve f in Fig. 6 is in good agreement with the experimental data while the CO conversion is >30% at high temperatures. Considering that (Fig. 6g) the coverage decreases before reaching 30% of CO conversion, it must be concluded that the difference between curves g and h is not mainly due to diffusion processes. This difference is probably related either to a modification of the elementary steps involved in the CO/O_2 reaction or to a change in the kinetic parameters involved in Model M1.

3.5. Rate of CO Oxidation during the Lighting-Off Tests

The rate of CO oxidation expressed as a turnover frequency (TOF) is given by (7, 26)

$$v_{CO} = k_3 \theta_L \theta_{O_{wads}}. \quad [8]$$

This rate is the average number of CO_2 molecules produced per active Pt atom per second (26).

Figure 1 shows that the CO conversion increases with the increase in the reaction temperature while θ_L either remains constant or decreases (mainly due to the adsorption equilibrium). To prevent the impact of diffusion processes, the comparison between theoretical and experimental TOF values (TOF_{ex} and TOF_{th}, respectively) must be performed

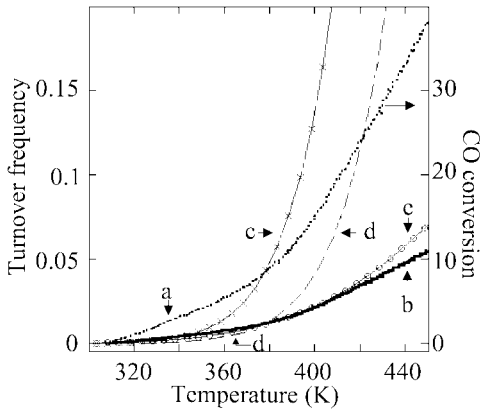

FIG. 7. Comparison of TOF_{ex} and TOF_{th} during a lighting-off test with 1% CO/0.25% O_2/He for low CO conversions: (a, b) CO conversion and TOF_{ex} with the quartz microreactor; (c, d) TOF_{th} according to Model M1, with $E_3 = 83$ and 87 kJ/mol, respectively; (e) TOF_{th} according to Model M1 considering that E_3 slightly increases with T_r (see the text).

at low CO conversion. The TOF_{ex} at the reaction temperature, T_r, is obtained from the molar fraction of either CO_2 ($X_{CO_2}(T_r)$) or CO obtained with the quartz microreactor, $TOF_{ex} = (X_{CO_2}(T_r) \cdot F/(W \cdot V_m \cdot N_s))$, where F is the flow rate, W the weight of catalyst, V_m the molar volume, and N_s the number of Pt sites involved in the reaction that is identified with the amount of adsorbed L CO species on the surface. The theoretical values of the TOF_{th} is obtained from expression [8]: θ_L and $\theta_{O_{wads}}$ are given by expressions [5] and [7], respectively, with the kinetic parameters used to obtain curves d and f in Fig. 6 except for the values of E_3, which is slightly modified to obtain the best fitting between TOF_{th} and TOF_{ex}. Curve b in Fig. 7 gives the TOF_{ex} values on the present Pt/Al_2O_3 catalyst for a 1% CO/0.25% O_2/He mixture. We have verified that this curve is not modified in the temperature range of Fig. 7, increasing the gas flow rate by a factor of 3. The TOF_{ex} values are in good agreement with that of Herz and Marin on Pt/Al_2O_3 (7). At $T = 473$ K the rate of oxidation is $\approx 1 \times 10^{-10}$ mol/(cm^2 of Pt $\times$ s) (see Fig. 1 in (7)) for high CO concentrations. Assuming 1×10^{15} site/cm^2, the TOF_{ex} in (7) is 0.06, as compared to 0.1 in the present study. Nibbelke *et al.* (5) find higher values on a Pt/Al_2O_3 catalyst for P_{CO}/P_{O_2} ratios >1 (see Fig. 2 in (5)): $\approx 4 \times 10^{-3}$ mol kg_{cat}^{-1} s^{-1} at 483 K. Considering a specific concentration of surface Pt of 8×10^{-3} mol kg_{cat}^{-1} (5), this provides a TOF of 0.5. Figure 7 compares TOF_{ex} (curve b) and TOF_{th} (curve c) for $P_{CO} = 1000$ Pa and $P_{O_2} = 250$ Pa for low CO conversions (curve a) using $E_3 = 83$ kJ/mol. A good agreement can be observed for CO conversion <5%. For high conversion values diffusion processes may limit the experimental rate of reaction ($TOF_{ex} < TOF_{th}$). The TOF_{th} values strongly increase with T_r, indicating a maximum of ≈ 1500 s^{-1} at 850 K. These values are on the order of magnitude of those measured for the CO/O_2 reaction by Oh *et al.* (26) on Rh(111), ≈ 1000 at 610 K, and by Su *et al.* (30) on Pt(111), 660 and 2685 at 640 and 750 K, respectively. However, they largely exceed the values needed to convert CO in the 1% CO/x% O_2/He mixtures. For instance, with a flow rate of 200 cm^3/min the amount of CO to be converted is 1.4 μmol/s. The number of Pt sites adsorbing the L species at 540 K on a stabilized solid is ≈ 70 μmol/g (13), leading to an average number of Pt sites for an experiment of ≈ 7 μmol. To convert totally CO, the TOF must be 0.2 molecule per site and per s, a value largely lower than the theoretical values. Herz and Marin (7) have performed a study similar to the present work, comparing theoretical (using kinetic parameters from UHV studies) and experimental rates of the CO/O_2 reaction on Pt/Al_2O_3 (from a study by Schlatter and Chou (31)). They consider two reaction models mainly differing by the activation of O_2 and they assume a competition between adsorbed CO and O species. This last point is one of the main differences with our model and prevents a full comparison between the two studies. However, the point of interest is that the authors (7) note a large difference between theoretical and experimental values of the rate of the CO/O_2 reaction even at low CO conversions while a good agreement is observed in Fig. 7. They have considered (7) that this difference was not due to mass transfer limitations and they have introduced a multiplying factor α ($\alpha = 1.77 \times 10^{-4}$) in their theoretical expression of the rate of reaction to represent the fraction of the surface metal atoms on the supported Pt catalyst that is active for the CO oxidation. The α value leads the authors to conclude that a very small fraction of the Pt atoms are in a reduced state and are active in the reaction (7). We cannot retain this explanation because (a) we consider that the intermediate in the CO/O_2 reaction is the L CO species adsorbed on the reduced Pt atoms and (b) a good agreement between TOF_{ex} and TOF_{th} is observed at low conversions (Fig. 7). We believe that in our case the large difference at high CO conversion is due to diffusion processes, as considered by Oh *et al.* (26). The authors have measured TOF values in the range 0.1–1000 on Rh(111) and in the range 1–20 on a 1% Rh/Al_2O_3 catalyst due to heat and mass transfer limitations on the supported Rh catalyst. The curve $TOF_{th} = f(T_r)$ presents a maximum at high temperatures due to the strong decrease in θ_L and $\theta_{O_{wads}}$. The presence of a similar high-temperature maximum in the rate of the CO/O_2 reaction has been observed at $T > 850$ K by Bald *et al.* (32) on a polycrystalline Pt solid.

The impact of E_3 on the curves $\theta_L = f(T_r)$ is limited (the main parameter affecting these curves is the heat of adsorption) while it is very important on $TOF_{th} = f(T_r)$. A change of a few kJ/mol leads to significantly different profiles. For instance, curve d in Fig. 7 is obtained with $E_3 = 87$ kJ/mol. Moreover, it has been shown in (1) that E_3 may slightly increase with the decrease in θ_L, as observed previously by Cant and Donaldson (33). A good agreement is observed between TOF_{ex} and TOF_{th} on a larger range of CO conversion if it is considered that E_3 slightly increases with an

increase in the reaction temperature (decrease in the coverage of the adsorbed species) from 83 kJ/mol at 320 K to 91 kJ/mol at 420 K, as observed in Fig. 7, curve e.

3.6. Comparison of the Present Conclusions on the CO/O_2 Reaction to Literature Data

Our approach to the CO/O_2 reaction from the surface elementary steps to a lighting-off test leads to the following conclusions concerning the kinetic order for CO and O_2 in an excess of CO: (a) the rate is almost independent of the partial pressure of CO because $\theta_{CO} \approx 1$ in a large temperature range (Fig. 6) and (b) the rate varies in $P_{O_2}^{0.5}$. The difficulty in the comparison of those conclusions with those coming from kinetic models in the literature on the CO/O_2 reaction on Pt/Al_2O_3 catalyst is that (a) usually a competitive adsorption between CO_{ads} and O_{ads} is assumed and (b) the same kinetic model tries to fit the experimental data in a large range of CO/O_2 ratios while we only consider an excess of CO. There are numerous studies dedicated to the kinetic of the CO/O_2 reaction on Pt-containing solids (3–8). However, to facilitate the presentation we compare the conclusions of the present study to a recent work on a 0.4% Pt/Al_2O_3 solid (5). Nibbelke *et al.* (5) have determined the rate of the CO oxidation on Pt/Al_2O_3 at 483 K showing the effects of P_{CO} at constant P_{O_2} values and of P_{O_2} at constant P_{CO} values. A reaction model has been proposed based on competitive adsorption between CO and O_2 with the adsorption of oxygen in two steps in series (irreversible molecular chemisorption in O_2^* followed by dissociation of O_2^*). With several assumptions, e.g., that (a) the adsorbed CO species is at the adsorption equilibrium (as observed in the present study), (b) the rate-determining step is O_2 chemisorption, and (c) the most abundant reaction intermediate is the adsorbed CO species (as observed in the present study), the authors find a rate expression (expression [13] in (5)) for the CO_2 production depending on P_{O_2} and P_{CO}^{-1}. The agreement between experimental and theoretical rates of reaction is good in excess O_2 while some differences are observed in excess CO (5). In particular, for CO/O_2 ratios >2, the authors show that the experimental kinetic order in O_2 is lower than 1 (see Fig. 2 in (5)). This is in good agreement with 0.5, determined with our procedure. Moreover, studying the effect of high P_{CO} values at a constant P_{O_2} value the authors clearly show that the experimental rate is roughly constant for $P_{CO}/P_{O_2} > 2$ (see Fig. 1 in (5)). This also is in good agreement with our conclusions that the kinetic order for CO is 0. Note that we consider that Model M1, which fits the curves $\theta_L = f(T_r)$ (Fig. 6) as well as $TOF_{ex} = f(T_r)$ for low CO conversions (Fig. 7), only is valid in an excess of CO. In particular, it cannot fit the curve $\theta_L = f(T_r)$ at high reaction temperatures for $P_{CO}/P_{O_2} = 2$ (Fig. 6). For P_{CO}/P_{O_2} ratios ≤ 2 a change in the surface elementary steps or/and the kinetic parameters must be involved in order to explain the kinetic orders for CO and O_2 determined by Nibbelke *et al.* (5). For the CO/O_2 reaction on a Pt foil at low total pressure ($<10^{-3}$ Pa), Golchet and White (34) have particularly shown the strong influence of the P_{CO}/P_{O_2} ratio on the kinetic orders of the CO/O_2 reaction. They have observed (see Fig. 5 in (34)) that at 620 K, the rate of the reaction is constant, increasing P_{CO} for CO/O_2 ratios >2, in agreement with our observations. However, the authors observed that at lower reaction temperatures the increase in P_{CO} leads to a slight inhibition of the reaction (negative order for CO). It was indicated in (2) that the pressure gap may lead to a situation where the reaction between L CO and O_{sads} species (step S3a) adsorbed on the same sites (competition) controls the CO_2 production at low pressure (UHV conditions) while step S3 controls the CO_2 production at high pressure with CO/O_2 ratios >2. This limits the comparison of the mechanism of CO/O_2 reaction obtained at high pressures (supported Pt catalysts) and UHV conditions (Pt single crystals and foils). Note that an inhibition by CO can be involved in Model M1 at high P_{CO} values by considering a competition between O_{wads} and the B CO species.

4. CONCLUSION

In the present study the evolutions of the coverage of the linear CO species θ_L and of the TOF for the CO/O_2 reaction on a 2.9% Pt/Al_2O_3 catalyst during lighting-off tests (an increase in the reaction temperature) performed with various 1% CO/x% O_2/He mixtures ($x \leq 0.5$) have been determined using FTIR and mass spectroscopy. The curves $\theta_L = f(T_r)$ as well as $TOF_{ex} = f(T_r)$ have been compared to those obtained from a kinetic model (denoted M1) for the CO/O_2 reaction in excess of CO.

Four elementary steps are involved in Model M1, forming a Langmuir–Hinshelwood mechanism: adsorption of CO (step S1) and of O_2 (step S2) to form L CO and weakly adsorbed, O_{wads}, species, respectively; surface reaction between L CO and O_{wads} (step S3); and desorption of CO_2 (step S4). The experimental curves $\theta_L = f(T_r)$ are very well interpreted considering that (a) there is an equilibrium on the Pt surface between the rate of adsorption of the L CO species and its rates of desorption and oxidation and (b) there is no competition between L and O_{wads} species. The O_{wads} species are probably formed on the Pt sites adsorbing the bridged CO species which has a low heat of adsorption. The kinetic parameters used in the M1 model are those previously determined by individually studying each surface elementary step. The heat of adsorption of the L species varies from 206 kJ/mol at $\theta_L = 0$ to 115 kJ/mol at $\theta_L = 1$. The oxygen species is weakly adsorbed, with a heat of adsorption $E_{O_2} \approx 30$ kJ/mol. The activation energy of step S3 is $E_3 \approx 85$ kJ/mol with a preexponential factor of $\approx 1 \times 10^{13}$ s^{-1}.

Experimental TOF values for the CO/O_2 reaction in excess of CO are in good agreement with theoretical values

for low CO conversions considering that the rate of the reaction is given by $v_{co} = k_3\theta_L\theta_{O_{wads}}$. The kinetic parameters are mainly those used to fit the curves $\theta_L = f(T_r)$. For high CO conversions, diffusion processes limit the rate of reaction. However, a good agreement between experimental and theoretical TOF values is observed on a larger CO conversion range considering a slight increase in E_3 with the decrease in the coverage of the adsorbed species.

The present model is not valid for CO/O_2 ratios ≤ 2 because in these conditions the surface elementary steps change or/and the kinetic parameters are modified. This is discussed in a forthcoming paper.

ACKNOWLEDGMENTS

We acknowledge with pleasure FAURECIA Industrie, Bois sur Prés, 25 550 Bavans, France, for its financial support and the MERT (Ministère de l'Education Nationale de la Recherche et de la Technologie) for the research fellowship of A. Bourane.

REFERENCES

1. Bourane, A., and Bianchi, D., *J. Catal*. **202**, 34 (2001).
2. Bourane, A., and Bianchi, D., *J. Catal.* **209**, 114 (2002).
3. Engel, T., and Ertl, G., *Adv. Catal*. **28**, 1 (1979).
4. Razon, L. F., and Schmitz, R. A., *Catal. Rev.–Sci. Eng*. **28**, 89 (1986).
5. Nibbelke, R. H., Campman, M. A. J., Hoebink, J. H. B. J., and Marin, G. B., *J. Catal*. **171**, 358 (1997).
6. Wojciechowski, B. W., and Aspey, S. P., *Appl. Catal. A* **190**, 1 (2000).
7. Herz, R. H., and Marin, S. P., *J. Catal*. **65**, 281 (1980).
8. Harold, M. P., and Garske, M. E., *J. Catal*. **127**, 524 (1991).
9. Chafik, T., Dulaurent, O., Gass, J. L., and Bianchi, D., *J. Catal*. **179**, 503 (1998).
10. Dulaurent, O., and Bianchi, D., *Appl. Catal*. **196**, 271 (2000).
11. Bourane, A., Dulaurent, O., and Bianchi, D., *J. Catal*. **196**, 115 (2000).
12. Bourane, A., Dulaurent, O., and Bianchi, D., *Langmuir* **17**, 5496 (2001).
13. Bourane, A., Dulaurent, O., and Bianchi, D., *J. Catal*. **195**, 406 (2000).
14. Kaul, D. J., and Wolf, E. E., *J. Catal*. **89**, 348 (1984).
15. Kaul, D. J., and Wolf, E. E., *J. Catal*. **93**, 321 (1985).
16. Anderson, J. A., *J. Chem. Soc. Faraday Trans*. **88**, 1197 (1992).
17. Haaland, D. M., and Williams, F. L., *J. Catal*. **76**, 450 (1982).
18. Barshad, Y., Zhou, X., and Gulari, E., *J. Catal*. **94**, 128 (1985).
19. Lindstrom, T. H., and Tsotsis, T. T., *Surf. Sci*. **150**, 487 (1985).
20. Schüth, F., Henry, B. E., and Schmidt, L. D., *Adv. Catal*. **39**, 51 (1993).
21. Cai, Y., Strenger, H. G., Jr., and Lyman, C. E., *J. Catal*. **161**, 123 (1996).
22. Glasstone, S., Laidler, K. J., and Eyring., H., "The Theory of Rate Processes." McGraw–Hill, New York/London, 1941.
23. Laidler, K. J., *Catalysis* **1**, 75 (1954).
24. Dulaurent, O., Chandes, K., Bouly, C., and Bianchi, D., *J. Catal*. **188**, 237 (1999).
25. Campbell, E. T., Ertl, G., Kuppers, H., and Segner, J., *J. Chem. Phys*. **73**, 5862 (1980).
26. Oh, S. H., Fischer, G. B., Carpenter, J. E., and Goodman, D. W., *J. Catal*. **100**, 360 (1986).
27. Lynch, D. T. L., Emig, G., and Wanke, S. E., *J. Catal*. **97**, 456 (1986).
28. Bonzel, H. P., and Burton, J. J., *Surf. Sci*. **52**, 223 (1975).
29. Kaul, D. J., Sant, R., and Wolf, E. E., *Chem. Eng. Sci*. **42**, 1399 (1987).
30. Su, X., Cremer, P. S., Ron Shen, Y., and Somorjai, G. A., *J. Am. Chem. Soc*. **119**, 3994 (1997).
31. Schlatter, J. C., and Chou, T. S., *in* "71st Annual Meeting, AIChE, November 1978," paper number 66f.
32. Bald, D. J., Kunkel, R., and Bernasek, S. L., *J. Chem. Phys*. **104**, 7719 (1996).
33. Cant, N. W., and Donaldson, R. A., *J. Catal*. **71**, 320 (1981).
34. Golchet, A., and White, J. M., *J. Catal*. **53**, 266 (1978).